

Total internal reflectance fluorescence (TIRF) biosensor for environmental monitoring of testosterone with commercially available immunochemistry: Antibody characterization, assay development and real sample measurements

Jens Tschmelak*, Michael Kumpf, Nina Käppel, Guenther Proll, Guenter Gauglitz

*Eberhard-Karls-University of Tuebingen, Institute of Physical and Theoretical Chemistry (IPTC),
Auf Der Morgenstelle 8, D-72076 Tuebingen, Germany*

Received 31 January 2005; received in revised form 22 June 2005; accepted 29 September 2005
Available online 21 November 2005

Abstract

Nowadays, little technology exists that can monitor various water sources quickly and at a reasonable cost. The ultra-sensitive, fully automated and robust biosensor River Analyser (RIANA) is capable of detecting multiple organic targets rapidly and simultaneously at a heterogeneous assay format (solid phase: bulk optical glass transducers). Commercialization of such a biosensor requires the availability of commercial high-affinity recognition elements (e.g. antibodies) and suitable commercial haptens (modified target molecules) for surface chemistry. Therefore, testosterone was chosen as model analyte, which is also a task of common analytical methods like gas chromatography–mass spectrometry (GC–MS), because they have to struggle with detecting sub-nanogram per liter levels in environmental samples. The reflectometric interference spectroscopy (RIfS) was used to characterize the commercially available immunochemistry resulting in a high-affinity constant of $2.6 \pm 0.3 \times 10^9 \text{ mol}^{-1}$ for the unlabeled antibody. After the labeling procedure, necessary for the TIRF-based biosensor, a mean affinity constant of $1.2 \times 10^9 \text{ mol}^{-1}$ was calculated out of RIfS ($1.4 \pm 0.4 \times 10^9 \text{ mol}^{-1}$) and TIRF ($1.0 \pm 0.3 \times 10^9 \text{ mol}^{-1}$) measurements.

Thereafter, the TIRF-based biosensor setup was used to determine the steroidal hormone testosterone at real world samples without sample pre-treatment or sample pre-concentration. Results are shown for rapid and ultra-sensitive analyses of testosterone in aqueous samples with at a remarkable limit of detection (LOD) of 0.2 ng L^{-1} . All real world samples, even those containing testosterone in the sub-nanogram per liter range (e.g. 0.9 ng L^{-1}), could be determined with recovery rates between 70 and 120%. Therefore, the sensor system is perfectly suited to serve as a low-cost system for surveillance and early warning in environmental analysis in addition to the common analytical methods. For the first time, commercially available immunochemistry was fully characterized using a label-free detection method (RIfS) and successfully incorporated into a TIRF-based biosensor setup (RIANA) for reliable sub-nanogram per liter detection of testosterone in aqueous environmental samples.

© 2005 Elsevier B.V. All rights reserved.

Keywords: Reflectometric interference spectroscopy (RIfS); Antibody characterization; Total internal reflectance fluorescence (TIRF); Environmental analysis; Testosterone; Steroidal hormones

1. Introduction

1.1. Environmental approach

The fast screening and monitoring of toxins in tap water, environmental samples, and food require new approaches in order to

expedite appropriate countermeasures. Many toxins in environmental samples can be introduced by industrial, agricultural, or even military activity. Pollutants, such as pesticides, hormones and other endocrine disrupting compounds (EDCs), also contaminate soil and ground water are known to show adverse or even toxic effects to humans at low nanogram per liter levels. Toxic compounds may also be found in environmental samples caused by terrorist activities. Therefore, home security and water safety require a very fast, cost-effective, and robust detection method for such compounds. Toxins also occur naturally in the food supply. Mycotoxin contamination is a particular

* Corresponding author. Tel.: +49 7071 29 74668; fax: +49 7071 29 5490.
E-mail address: jens.tschmelak@ipc.uni-tuebingen.de (J. Tschmelak).
URL: <http://barolo.ipc.uni-tuebingen.de>.

problem due to fungal infection of grains and peanuts and can still be present after food processing [24]. Whereas many cases of food borne illnesses are caused by bacteria, a large number of illnesses are also caused by bacterial toxins that have been secreted into the foodstuff during growth [2]. Agricultural products can also be contaminated with pesticides, which may be toxic to humans. In all, hormones and other EDCs, whereas testosterone was used as model analyte, have adverse effects on aquatic communities and human beings. A huge amount of natural hormones and endocrine disrupting chemicals are reaching surface waters [6,11,23]. The main sources of this pollution are wastewater treatment plants and intensive stock rearing. The effects of estrogenic compounds and of whose mixtures are not entirely clear, but a no effect concentration (NOEC) or a lowest observable effect concentration (LOEC) in the lower nanogram per liter range is often discussed in literature [14,21,26,34]. The NOEC for vitellogenin in fish has been tested in numerous species [1,9,19,20,29,30]. It does not matter, if there is an acute or chronic aquatic toxicity, the intention should be clear. What we need is a secure and accurate detection of problematic compounds at low nanogram per liter levels in various water matrices. For common analytical methods, it is necessary to pre-concentrate samples by orders of magnitude to reach detectable amounts of the analytes [16], but analytical methods at a very low limit of detection (LOD) and a low limit of quantification (LOQ) for problematic compounds in water are very important in environmental analysis [10]. Promberger and Schmid [18] reported about the determination of endocrine disruptors in drinking and ground water in Austria by gas chromatography–mass spectrometry (GC–MS) [18]. For this commonly used method, they reported LOQs for 21 endocrine active substances ranging from 3 to 1100 ng L⁻¹ and the LOQ for testosterone was 10 ng L⁻¹. As we know from a water investigation institute, conventional water analysis (GC–MS) can quantify testosterone at levels of 1–5 ng L⁻¹ after sample enrichment of several orders of magnitude (solid-phase extraction with a factor of 10,000: starting with 1 L water and ending up with 100 µL organic solvent) and testosterone derivatization before injection into the instrument. The time-consuming and expensive procedure of this problematic analysis leads to errors of at least 30 up to 50% in the lower nanogram per liter range.

1.2. Clinical aspects

Varieties of immunological methods are used to determine testosterone levels in serum, which serves as important diagnostic marker in humans [13,32]. The absolute serum testosterone concentration are useful in evaluating patients with polycystic ovary syndrome, hyperandrogenic women with clinical manifestations of hirsutism, acne and alopecia, in postmenopausal women with androgen deficiency, and in men with hydrogonadism. In addition, testosterone is measured in many studies like epidemiologic studies of breast and prostate cancers. Testosterone immunoassays (chiefly competitive assays) utilize radioactive, chemiluminescent, colorimetric or fluorescent markers. These assays are performed with or without preceding purification of the analyte. Only the non-radioactive are now

used widely in automated systems. Several studies have evaluated the reliability of measuring endogenous testosterone levels directly in serum or plasma by using manually or automated commercially available immunoassays [3,5,31,33]. Taieb et al. [25] compared 10 immunoassays for human (men, women, and children) sera testosterone with a common analytical method (GC–MS). The background of this study was that commercially available testosterone immunoassays give divergent results, especially at the low concentrations seen in women. The methods used, were eight non-isotopic immunoassays, two isotopic immunoassays, and isotope-dilution gas chromatography–mass spectrometry. Seven out of 10 immunoassays overestimated testosterone concentrations in samples of women in comparison to the common analytical method. Furthermore, the immunoassays underestimated testosterone levels in samples from men. They concluded that none of the immunoassays tested was sufficiently reliable for the investigation of sera from children and women, in whom very low or low testosterone concentrations (0.17–1.7 nmol L⁻¹ or 49–490 ng L⁻¹, respectively) are expected.

1.3. Research needs

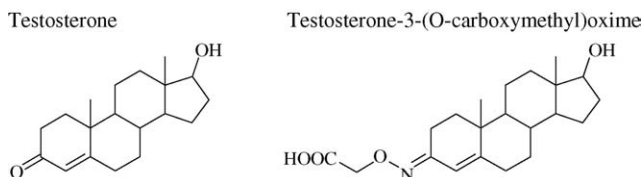
Having in mind the needs, described in the previous two chapters, of environmental and clinical analysis the research needs are clear. Up to now, cost-effective and ultra-sensitive monitoring of testosterone in water resources is not possible by using common analytical methods with their time-consuming sample pre-treatment and pre-concentration. Likewise, improved immunological methods for testosterone detection in biological fluids are needed to compete with common analytical instruments in clinical laboratories. Our fully automated immunosensor with its capability to measure estrone below the important NOEC is a perfectly suited instrument to serve as a low-cost system for surveillance and early warning in environmental analysis [27]. The River Analyser (RIANA) was successfully used for heterogeneous non-competitive immunoassays involving fluorescent-labeled molecular recognition elements (e.g. polyclonal or monoclonal antibodies) detecting organic pollutants in aqueous samples (chiefly different water types) via binding inhibition assays. Nowadays, commercially available immunochemistry should be used on the RIANA system to allow ultra-sensitive testosterone detection in water samples. The use of commercial products guarantees the broad usability of this newly developed assay. First, the available immunochemistry should be characterized via a label-free detection method. The biosensor used for antibody characterization is based on reflectometric interference spectroscopy (RIfS) using multiple reflection at thin layers [17]. By using this method, it is possible to get information about the kinetics and thermodynamics of the observed process as well as of the concentration of active antibody in bulk solution. This allows us, to crosscheck the affinity constant of the anti-testosterone towards the promised affinity by the supplier and to observe the labeling-process with respect to degradation and alteration of the monoclonal antibody used. After obtaining maximum value out of the determined kinetic and thermodynamic data, the development of a fluorescence-

based immunoassay for ultra-sensitive testosterone detection should be no problem. Verifying the assay performance in real world samples using our immunosensor with spiked river and drinking water at different levels of testosterone, should result in recovery rates between 70 and 120%, as the AOAC International recommends it [15]. The next step should include biological fluids like urine and serum, or even plasma. The immunoassay and the instrument used must be adjusted to the exigencies of these complex matrices.

2. Experimental

2.1. Materials

The steroidal hormone testosterone (17 β -hydroxy-4-androsten-3-one) was purchased as VETRANAL[®] analytical standard from Riedl-de Haën Laborchemikalien GmbH & Co. KG, Seelze, Germany. The fluorescent dye CyDye[™] Cy5.5 was purchased from Amersham Biosciences, Europe GmbH, Fribourg, Germany. The aminodextrans Amdex[™] with 40 and 170 kDa molecular weight were purchased from Helix Research Company, Springfield, OR, USA. The monoclonal antibody to testosterone (catalog no. BM2076, clone 7003, host mouse, isotype IgG1, immunogen: T-3-CMO-BSA) was purchased from Acris Antibodies GmbH, Hiddenhausen, Germany. The derivative testosterone-3-(*O*-carboxymethyl)oxime (17 β -hydroxy-4-androsten-3-one-3-(*O*-carboxymethyl)oxime) used for surface chemistry is commercially available, for instance, from Sigma–Aldrich Chemie GmbH, Steinheim, Germany (product no. T8390, CAS 10190-93-9, molecular formula C₂₁H₃₁NO₄, molecular weight 361.5). Labeling and purification of the monoclonal antibody were carried out as described in the product information sheet supplied with the labeling kit from Amersham Biosciences, Europe GmbH, Fribourg, Germany. UV–vis spectra were recorded using a Specord M500 spectrophotometer from Carl Zeiss Jena GmbH, Jena, Germany. Common chemicals of analytical grade were purchased from Sigma–Aldrich Chemie GmbH, Steinheim, Germany, or Merck KGaA, Darmstadt, Germany.



2.2. Methods

2.2.1. RfS—characterization setup

The biosensor used for antibody characterizations is based on reflectometric interference spectroscopy using multiple reflection at thin layers. Therefore, white light is guided with an optical fiber to the transduction layer. At each interface between different refractive indices, the light is partially reflected. These reflected beams superimpose and build a characteristic interference spectrum, which is detected with a diode-array. The binding

of antibodies to the surface changes the optical thickness of the toggling layer, which causes a change in the reflectance spectrum. Thus, the interaction process between the antibody and the hapten derivative on the surface can be detected time-resolved and label-free. A scheme of the detection method is shown in Fig. 1. With this method, it is possible to get information about the kinetics and thermodynamics of the observed process as well as of the concentration of active antibody in bulk solution. The RfS setup is described in detail in the work of Schmitt et al. [22].

All samples measured with RfS were handled by a commercial flow system (Automated Sample Injection Analyser—ASIA from Ismatec, Wertheim-Mondfeld, Germany), which contains two peristaltic pumps and a six-way valve. Moreover, this flow system is equipped with an auto sampler from Ismatec, Wertheim-Mondfeld, Germany. The auto sampler was used to inject the samples into a sample loop. From there, the sample is driven in continuous flow passing the prepared transducer. After the interaction process, the transducer surface is regenerated with 0.5% sodium dodecyl sulfate (SDS) at pH 2. This procedure does not destroy the immobilized hapten derivative, but cleans the surface from bound antibody.

2.2.2. TIRF—measurement setup

The setup of the River Analyser is well described by Tschmelak et al. [27] and consists of the following components. Light from a laser diode (Coherent Deutschland GmbH, Dieburg, Germany) with approximately 15 mW operating at 635 ± 2 nm is coupled into the beveled edge of a bulk optical glass slide (Schott Spezialglas GmbH, Gruenenplan, Germany). The laser beam is guided by total internal reflection along the sensitive area of the glass transducer. Fluorescent dyes close to the chip surface are excited by the evanescent field at the reflection spots. The emitted fluorescence light is collected via polymer fibers, filtered by absorption filters with cut-on at 690 nm (Omega[®] Optical Inc., Brattleboro, VT, USA), detected by photodiodes using lock-in detection and the signals are electronically amplified before data recording. An HTS PAL auto sampler with cycle composer software (CTC Analytics AG, Zwingen, Switzerland) is used for dilutions, sample preparations (transferring 100 μ L of the antibody stock solution to 900 μ L of the sample followed by two mixing strokes) and the sample transfer to the River Analyser. Liquid handling and data acquisition are fully automated and computer-controlled. One measurement cycle with washing steps, injection of the sample and regeneration of the surface takes about 12 min. The regeneration protocol consists of a flow cell flushing with 400–800 μ L of a diluted SDS solution (0.5% SDS in Milli-Q water at pH 2) followed by a rinsing step with buffer. Such a regeneration cycle can be repeated up to 1000 times depending on the stability of the immobilized analyte derivatives on the transducers. Afterwards, the transducers can be recycled by starting the surface chemistry (see Section 2.2.4) from the beginning.

2.2.3. Assay format

The test format used for all measurements is a binding inhibition assay. Here, an analyte derivative (analyte molecule mod-

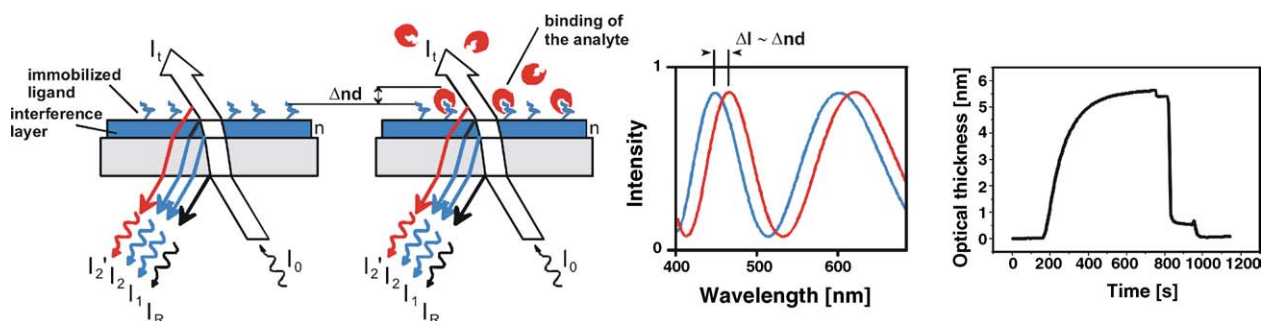


Fig. 1. Scheme of the RfS detection method. The left part of the scheme shows how the reflected beams superimpose and how the optical thickness of the transducer changes during binding events onto the surface. The right part shows the change of the characteristic interference spectrum and how this shift is transformed into a signal curve.

ified with a spacer containing a carboxyl group) is covalently immobilized to an aminodextran layer bound to the glass transducer. This aminodextran layer is used to reduce non-specific binding to the surface. The sample containing the analyte is incubated in solution with the specific antibody. Therefore, 100 μL of the antibody stock solution are mixed with 900 μL of the sample and are incubated for approximately 5 min. The antibody binds the analyte during the incubation step until the equilibrium of the reaction is reached. When the sample is pumped over the sensor surface, only the antibodies with free paratopes can bind to the surface. For the binding inhibition assay to be quantitative, the binding of the antibody to the surface must be mass transport-limited. This allows the signal to be a function of rather the diffusion rate to the surface than of the kinetics of the surface binding. To this purpose, the number of high-affinity binding sites on the surface has to be much higher than the number of antibodies in bulk solution. To be sure that the binding is mass transport-limited, we use small amounts of antibodies and we immobilize a huge excess of antigen derivatives on the sensor surface. The binding inhibition assay was carried out in single analyte operating state.

2.2.4. Immobilization strategies

RfS-transducer chips of 1 mm D 263 glass with layers of 10 nm Nb_2O_5 and 330 nm SiO_2 (Unaxis AG, Pfäffikon, Switzerland) were cleaned with freshly prepared Piranha solution (mixture of 30% hydrogen peroxide and concentrated sulphuric acid at a ratio of 2:3) for 30 min in an ultrasonic bath. After rinsing with Milli-Q water and drying in a nitrogen stream, the surface was immediately activated by (3-glycidyloxypropyl)trimethoxysilane (GOPTS) for 1 h in dryness followed by cleaning with dry acetone and drying in a nitrogen stream. The coupling of aminodextran (AmdexTM with 170 kDa molecular weight with 1 amino group per 13 glucose units) as an aqueous solution (1:3) to this silanized surface is carried out by incubating for 4 h in a water-saturated atmosphere. After thoroughly rinsing with Milli-Q water and drying, the prepared chips are stable for several months. The covalent coupling of the testosterone derivative testosterone-3-(*O*-carboxymethyl)oxime (which carries a carboxylic group) to this modified transducer surface is done by an activated ester, generated by *N,N'*-dicyclohexylcarbodiimide (DCC) in dry *N,N*-dimethylformamide (DMF). The reaction is finished after 1 h,

and then, the transducers are rinsed with DMF and Milli-Q water before being dried in a nitrogen stream. These treated transducers carry specific binding sites for the testosterone antibody with a high density and can, therefore, serve as a sensor surface. In addition, the aminodextran coating used reduces unspecific binding to this surface.

The bulk optical glass transducers for TIRF measurements were cleaned in the same way as described for the smaller RfS-transducers. After drying under a nitrogen flow, 25 μL of (GOPTS) were applied to the surface and reacted for 30 up to 60 min. The silanized surface was rinsed with dry acetone and dried under a flow of nitrogen. Subsequently, the dissolved aminodextran (AmdexTM with 40 kDa molecular weight with 1 amino group per 11 glucose units) was applied to this silanized surface and incubated for up to 5 h in a water-saturated atmosphere. Thereafter, the testosterone derivative is immobilized in the same way as previously described for the RfS-transducer chips.

2.3. Measurement and data evaluation

2.3.1. RfS

As described in Section 2.2.3, the measurements have to be performed under mass transport-limited conditions. To this purpose, the antibody concentration was adjusted to a slope of 1 pm optical thickness per second. This concentration depends on the flow channel, the flow velocity, and most of all on the activity of the antibody.

The concentration of monoclonal bivalent antibody with free paratopes can be calculated using the law of mass action and assuming that both paratopes are independent to:

$$c_{R,f} = \frac{c_R}{2} - \frac{\left(\frac{c_R + c_L + K^{-1}}{2} - \sqrt{\frac{1}{4}(c_R + c_L + K^{-1})^2 - c_R c_L} \right)^2}{2 c_R},$$

with the concentration of free antibody (receptor), $c_{R,f}$, the concentration of antibody binding sites, c_R , the concentration of analyte (ligand), c_L and the affinity constant, K [17]. Normally, the relative free antibody, $c_{R,f}/2c_R$, is plotted to the concentration of analyte, c_L . Adjusting the resulting formula by a Levenberg–Marquardt least square fit to the measured values, the affinity constant and the active antibody concentration can

be determined. This approximation fits well for the unlabeled antibody, but for the fluorescence labeled antibody the assumptions of being monoclonal and independent reaction of the two binding sites is not true. Therefore, the determination of the active concentration and the affinity constant is different.

The active concentration of the fluorescence labeled antibody is evaluated by comparing the slope of a sample of unlabeled antibody with known activity with the slope of a sample of labeled antibody, whereas both samples contain the same amount of protein. The affinity of the antibody–analyte reaction can be determined by approximating the data with the logistic fit function (see Section 2.3.2) and determining the concentration of analyte, which remains half of the antibodies to have a free binding site. This concentration yields the equation:

$$K = \frac{2 + \sqrt{2}}{\sqrt{2}c_{L,0.5} - c_R},$$

where $c_{L,0.5}$ is analyte concentration and half of the antibodies are free, c_R the concentration of antibody binding sites and K is the affinity constant [17]. For the logistic fit function, $c_{L,0.5}$ is equal to the variable x_0 .

To determine the activity and the affinity constant of a labeled and unlabeled anti-testosterone antibody, we performed measurements with 450 ng mL⁻¹ antibody and variable amounts of testosterone ranging from 0.9 ng L⁻¹ to 900 µg L⁻¹. The comparison of the different slopes was performed with the same amount of antibody. These measurements are displayed in Fig. 2.

2.3.2. TIRF

For the measurements, we used labeled (CyDye Cy5.5TM) monoclonal IgG1 antibody from mouse and the suitable analyte derivative (testosterone-3-(*O*-carboxymethyl)oxime). The entire sample volume was 1000 µL. For a calibration routine, 900 µL of spiked Milli-Q water was automatically mixed by the auto sampler with 100 µL of a cooled antibody stock solution (approximately, 6–8 °C) containing the labeled antibody and ovalbumin from chicken eggs (OVA) in 10-fold phosphate buffered saline (PBS) (10-fold PBS: pH 6.8, 1500 mM sodium chloride, 100 mM potassium phosphate monobasic). After a defined incubation time of approximately 5 min, this mixture was measured using the biosensor setup. The experimental design for a calibration routine consists of nine independent blank (Milli-Q water) measurements and eight concentration steps (each measured as three replica) of the analyte (spiked Milli-Q water). For all concentration steps and the blank measurements (nine replica), the mean value and the standard deviation (S.D.) for the replica was calculated. The measured signal for the mean value of the blanks was set to 100% and all spiked samples could be obtained as a relative signal below this blank value. To fit the data set, a logistic fit function [4] (parameters of a logistic function: A_1 , A_2 , x_0 , and p) was used:

$$y = \frac{A_1 - A_2}{1 + (x/x_0)^p} + A_2.$$

where A_1 is the upper asymptote and A_2 is the lower asymptote. The range between A_1 and A_2 is the dynamic signal range. The inflection point is given by the variable x_0 and represents the

analyte concentration, which corresponds to a decrease of 50% of the dynamic signal range (IC₅₀). The slope of the tangent in this point is given by the parameter p . Out of the logistic fit data, the 10–90% range of the dynamic signal can be calculated which gives an first impression about the possible utilizable range of the received calibration curve. In compliance with the IUPAC rules (The Orange Book) [8], the limit of detection (LOD) is calculated as three times the S.D. of the blank measurements (S.D._{blanks}) and the limit of quantification (LOQ) is calculated as 10 times the S.D._{blanks}. The use of LOQ for logistic calibration curves is skeptical, because with its non-linear behavior, the results for immunoassays are often worse than they need to be. A real alternative is the use of the 95% confidence belt and the related minimum detectable concentration (MDC) and reliable detection limit (RDL) [28]. O'Connell et al. [28] reported on calibration and assay development using the four-parameter logistic model and assay quality control procedures. We used Origin 7G SR4 (OriginLab Corporation, Northampton, MA, USA) to fit the data set and to calculate the 95% confidence belt. The received data were used to calculate the validation parameters LOD, LOQ, MDC, and RDL. All important statistical calculations of the data evaluation were done in a semi-automated procedure.

To determine the working range, the precision profile ($x_{cv,i}$) and its intersections with the Horwitz curve [7,12] has to be calculated. Based on scores of AOAC inter-comparison programs, Horwitz developed an empiric correlation between the comparative standard deviation and the concentration. For laboratory inter-comparison programs, Horwitz proposed an equation for the reproducibility $\sigma_R = fc^{0.8495}$ with a factor $f=0.02$. The corresponding error is the relative standard deviation R.S.D. = $100 \times (\sigma_R/c)$ that can be calculated with the reproducibility σ_R and the analyte concentration c . For intra-laboratory reproducibility, Horwitz found a higher precision and consequently lower R.S.D. values. In this case, the factor f can be reduced to two-thirds up to half of its former value. R.S.D. values can be calculated for each concentration and they represent the Horwitz curve (see Figs. 2–5). A valid concentration determination is possible only if the precision profile is below the Horwitz curve. The S.D. values of the inverse function (S.D. _{x_i}) can be calculated using the S.D. values of the measured data (S.D. _{y_i}) and the associated values of the first derivative (y') of the logistic fit (y) for each concentration. Then, the variation coefficients ($x_{cv,i}$) can be calculated and plotted together with the values of the Horwitz curve and the calibration data in the semi-logarithmic graph. Finally, the range between the intersection points of the Horwitz curve and the precision profile as can be seen in Figs. 2–5 gives the working range.

3. Results

The use of antibodies in immunochemistry requires high-affinity to a certain analyte. In our model system, the commercial available monoclonal antibody anti-testosterone yields this requirement with an affinity constant of $2.6 \pm 0.3 \times 10^9$ mol⁻¹ for an unlabeled antibody. This value was calculated from the data displayed in Fig. 2 using the equation in Section 2.3.1.

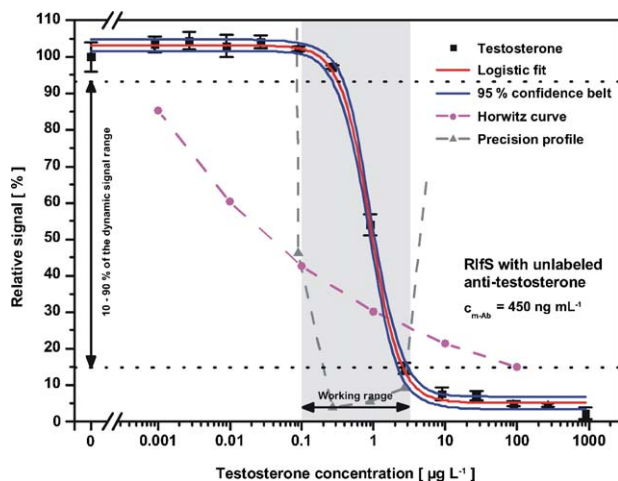


Fig. 2. Testosterone calibration curve using the RIfS detection method showing measured values for an unlabeled antibody with an affinity constant of $2.6 \pm 0.3 \times 10^9 \text{ mol}^{-1}$ and an active antibody concentration of approximately 50.8%.

Moreover, the activity of the antibody was determined with 50.8%. During the labeling procedure, the antibody losses further 45% of its activity, so only 27.4% of the labeled antibody is active. Using this antibody concentration, the affinity of the labeled antibody can be determined to $1.4 \pm 0.4 \times 10^9 \text{ mol}^{-1}$ using the data shown in Fig. 3 with the method RIfS and to $1.0 \pm 0.3 \times 10^9 \text{ mol}^{-1}$ with the method TIRF (see Fig. 4). The calculated affinities (RIfS and TIRF) of the labeled antibody are very similar resulting in a mean value of approximately $1.2 \times 10^9 \text{ mol}^{-1}$. The parameters of the logistic fit and validation parameters are summarized in Table 1. The decreased affinity can be explained due to the labeling procedure of the monoclonal antibody that results in a quasi-polyclonal labeled antibody. Triplicate UV-measurements from 240 to 800 nm have determined a mean dye to antibody rate of 2.6 calculated according to the product information sheet of the labeling kit used.

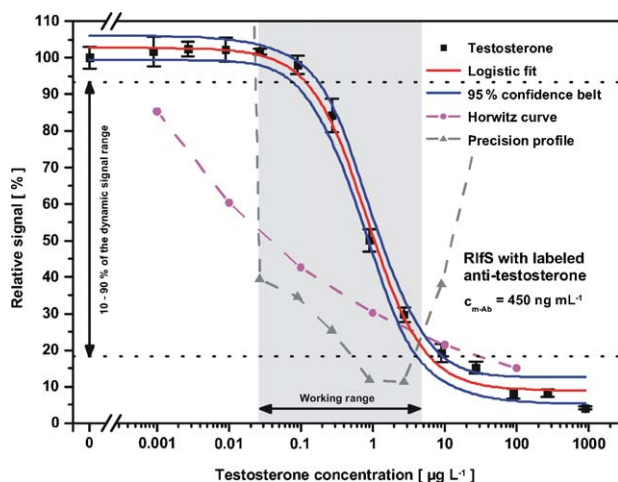


Fig. 3. Testosterone calibration curve using the RIfS detection method showing measured values and the logistic fit, which result in an affinity constant of $1.4 \pm 0.4 \times 10^9 \text{ mol}^{-1}$ with a previously determined activity of approximately 27.4%.

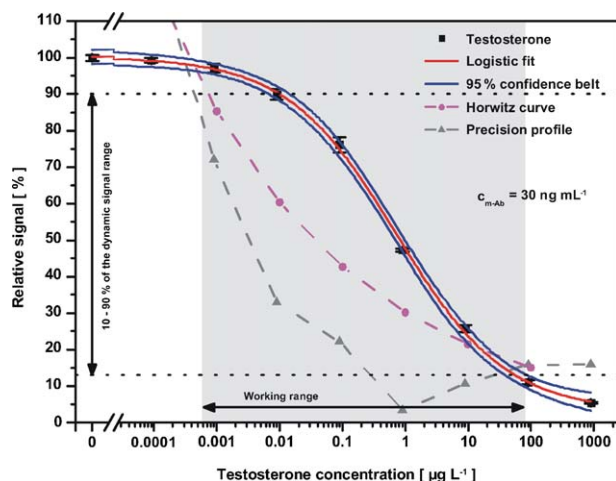


Fig. 4. TIRF-based calibration curve and 95% confidence belt for testosterone measured on a testosterone-3-(O-carboxymethyl)oxime (derivative) modified transducer from 90 pg L^{-1} to $900 \mu\text{g L}^{-1}$ (eight steps). The antibody (first batch) concentration (c_{m-Ab}) was 30 ng mL^{-1} in each sample. The working range from approximately 0.6 ng L^{-1} to $80 \mu\text{g L}^{-1}$ is shaded in gray.

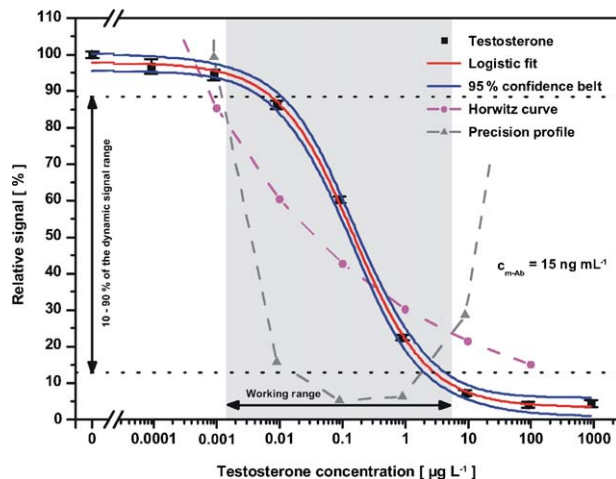


Fig. 5. TIRF-based calibration curve and 95% confidence belt for testosterone measured on a testosterone-3-(O-carboxymethyl)oxime (derivative) modified transducer from 90 pg L^{-1} to $900 \mu\text{g L}^{-1}$ (eight steps). The antibody (second batch) concentration (c_{m-Ab}) was 15 ng mL^{-1} in each sample. The working range from approximately 1.5 ng L^{-1} to $5.5 \mu\text{g L}^{-1}$ is shaded in gray.

Table 1

Parameters of the logistic fit function (A_1 , A_2 , x_0 , and p) including errors (S.D. A_1 , S.D. A_2 , S.D. x_0 , and S.D. p) and validation parameters (LOD, LOQ, MDC, and RDL) for all four calibration curves (RIfS and TIRF) with the different antibody concentrations (c_{AB}) between 15 and 450 ng mL^{-1} of anti-testosterone

Detection method	RIfS	RIfS	TIRF	TIRF
$c_{AB} [\text{ng mL}^{-1}]$	450 ^a	450 ^b	30 ^b	15 ^c
$A_1 [\%]$	103.1 ± 0.7	102.8 ± 1.5	100.2 ± 0.8	97.8 ± 0.9
$A_2 [\%]$	5.2 ± 0.8	9.0 ± 1.7	3.1 ± 1.3	3.4 ± 1.0
$x_0 [\mu\text{g L}^{-1}]$	0.91 ± 0.03	0.85 ± 0.08	0.72 ± 0.07	0.15 ± 0.01
p	2.11 ± 0.16	1.11 ± 0.11	0.50 ± 0.02	0.74 ± 0.04
LOD [ng L^{-1}]	405.5	149.6	0.6	0.2
LOQ [ng L^{-1}]	808.7	492.3	6.6	5.2
MDC [ng L^{-1}]	129.6	43.3	0.3	0.9
RDL [ng L^{-1}]	193.2	85.7	1.0	2.2

^a Unlabeled anti-testosterone from first batch.

^b Labeled anti-testosterone from first batch (dye to antibody rate of 2.6).

^c Labeled anti-testosterone from second batch (dye to antibody rate of 2.4).

We used testosterone as example to adapt the first commercially available assay on our TIRF-based biosensor RIANA. Therefore, the characterized labeled antibody with an affinity constant of $1.2 \times 10^9 \text{ mol}^{-1}$ was incorporated into a heterogeneous non-competitive immunoassay. In a first step, a freshly prepared transducer with the derivative testosterone-3-(*O*-carboxymethyl)oxime immobilized on the complete sensitive area of the chip was calibrated with testosterone from 90 pg L^{-1} to $900 \mu\text{g L}^{-1}$ in eight steps by using 30 ng labeled anti-testosterone (protein amount with an activity of 27.4%) per sample (sample volume: 1.0 mL). The calibration resulted in a LOD of 0.6 ng L^{-1} , a LOQ of 6.6 ng L^{-1} , a MDC of 0.3 ng L^{-1} , and RDL of only 1.0 ng L^{-1} . The resulting calibration curve is shown in Fig. 4 and all parameters of the logistic fit function and calculated results for the validation parameters are summarized in Table 1. The 10–90% range of the dynamic signal starts at 9.4 ng L^{-1} and ends at $54.9 \mu\text{g L}^{-1}$. In contrast, the working range depending on the Horwitz curve and precision profile starts at 0.6 ng L^{-1} (which is equivalent to the LOD) and ends at $80 \mu\text{g L}^{-1}$ after over five orders of magnitude. To get a first impression about real world testosterone quantification using our immunosensor, we spiked drinking water (Tuebingen, Germany) at two different testosterone levels (45 and 90 ng L^{-1}). The obtained data for triplicate measurements have been evaluated using the corresponding calibration curve (see Fig. 4) and parameters of the corresponding logistic fit (see Table 1), respectively. Out of these evaluated results, we calculated mean recovery rates as percentage of testosterone contamination. The recovery rates could be obtained at $75.0 \pm 9.6\%$ for the lower spiking level and $108.3 \pm 13.8\%$ for the higher spiking level. The results are shown in Fig. 6 together with following real world sample measurements.

Due to the poor activity of only 27.4% of the labeled anti-testosterone (see above), we ordered a second batch of this

antibody. A smoother labeling procedure (shorter reaction time, lower temperature, smaller volume) resulted in a mean dye to antibody rate of 2.4 calculated according to the product information sheet via triplicate UV-measurements from 240 to 800 nm. Having in mind the recently published results about the effects of reducing the amount of antibody within TIRF-based immunoassays [27], the same TIRF-transducer was calibrated with testosterone from 90 pg L^{-1} to $900 \mu\text{g L}^{-1}$ in eight steps by using only 15 ng labeled anti-testosterone per sample. The calibration resulted in a LOD of 0.2 ng L^{-1} , a LOQ of 5.2 ng L^{-1} , a MDC of 0.9 ng L^{-1} , and RDL of only 2.2 ng L^{-1} . As expected, the LOD and LOQ of this second calibration were improved by using half of the labeled antibody (second batch). Only the accuracy of the logistic fit suffers from the antibody reduction. Therefore, the 95% confidence belt is wider and consequently MDC and RDL show higher values. The 10–90% range of the dynamic signal starts at 7.4 ng L^{-1} and ends at $2.9 \mu\text{g L}^{-1}$ (see Fig. 5), which is remarkable smaller than for the first TIF-based calibration curve shown in Fig. 4, as well as the working range depending on the Horwitz curve and precision profile which lasts from 1.5 ng L^{-1} to $5.5 \mu\text{g L}^{-1}$. The second TIRF-based calibration curve with only 15 ng labeled anti-testosterone is shown in Fig. 5 and all parameters of the logistic fit function and calculated results for the validation parameters are summarized in Table 1. To ensure high-precision testosterone quantification at real world sampling using our immunosensor, we spiked lab water (Milli-Q), drinking water (Tuebingen, Germany) and river water (River Neckar, Germany) at three different testosterone levels. We started close to LOD and MDC at only 0.9 ng L^{-1} although this spiking level is not within the working range from 1.5 ng L^{-1} to $5.5 \mu\text{g L}^{-1}$. The two other spiking levels were 9 and 90 ng L^{-1} to verify a precise determination of high contamination levels. The obtained data for triplicate measurements, with only 0.7–2.1% error in relative signal scale, has been evaluated using the corresponding calibration curve (see Fig. 5) and parameters of the corresponding logistic fit (see Table 1), respectively. Out of these evaluated results, we calculated mean recovery rates as percentage of testosterone contamination. The recovery rates could be obtained between 78.4 and 118.2% with errors between 4.9 and 20.0%. Therefore, all mean recoveries could be obtained between 70 and 120%, as it is recommended by the AOAC International [15]. The results for recovery rates are summarized in Fig. 6.

4. Conclusions: an outlook

The RIfS setup is able to characterize an antibody completely. Not only in his affinity, assuming that the protein concentration is equal to the active concentration; moreover, the activity can be determined. Furthermore, once characterized monoclonal antibody to an analyte, any other polyclonal or monoclonal antibody to the same analyte can be characterized and compared to this first (monoclonal) antibody. Moreover, it was shown that the fluorescent label has no effect on the method RIfS and delivers the same results as TIRF measurements. The decreased affinity and the loss of activity of the labeled antibody compared to the unlabeled antibody can be explained due to the labeling procedure

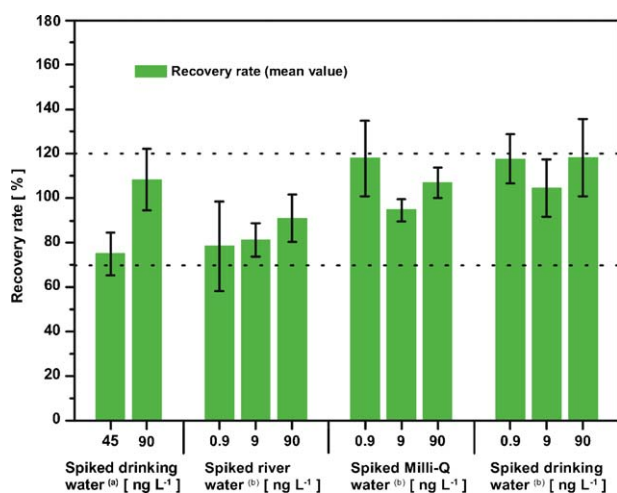


Fig. 6. This chart shows mean recovery rates with error bars (triplicate determination) for different water matrices (lab water (Milli-Q), drinking water (Tuebingen, Germany), and river water (River Neckar, Germany)) at various spiking levels. Recovery rates for the TIRF-based testosterone calibration with: (a) 30 ng labeled anti-testosterone (see Fig. 4) and (b) 15 ng labeled anti-testosterone (see Fig. 5).

of the monoclonal antibody, which results in quasi-polyclonal labeled antibody.

For the first time, commercially available immunochemistry was successfully implemented on the TIRF-based biosensor River Analyser resulting in a LOD of only 0.2 ng L^{-1} for direct measurements of water samples. To verify high-precision and robust testosterone quantification at real world sampling using our immunosensor, we spiked lab water (Milli-Q), drinking water (Tuebingen, Germany) and river water (River Neckar, Germany) at different testosterone levels. All real water samples, even those containing testosterone in the sub-nanogram per liter range (e.g. 0.9 ng L^{-1}), could be determined with recovery rates between 70 and 120%. Therefore, the sensor system is perfectly suited to serve as a low-cost system for surveillance and early warning in environmental analysis in addition to the common analytical methods. Now, our immunoassay and the instrument should be transferred to clinical analysis to measure testosterone in biological fluids like urine, serum, or plasma.

Acknowledgements

The main part of this work was funded by the “Automated Water Analyser Computer Supported System—AWACSS” (EVK1-CT-2000-00045) research project supported by the European Commission under the Fifth Framework Program and contributing to the implementation of the Key Action “Sustainable Management and Quality of Water” within the Energy, Environment and Sustainable Development. Another part of this work has been supported by the Bundesministerium fuer Bildung und Forschung (BMBF) within the “Parallelisiertes Immunreaktionsbasiertes Wasser-Analysator-System—PIWAS” (FK-02WU0243-6) project. The development of the biosensor used was funded by the European Commission under the Environment and Climate Program River Analyser (ENV4-CT95-0066) project. Jens Tschmelak is a scholarship holder, Michael Kumpf, and Guenther Proll are participants of the research training group “Quantitative Analysis and Characterization of Pharmaceutically and Biochemically Relevant Substances” funded by the Deutsche Forschungsgemeinschaft (DFG) at the Eberhard-Karls-University (EKU) of Tuebingen.

References

- [1] B. Allner, G. Wegener, T. Knacker, P. Stahlschmidt-Allner, *Sci. Total Environ.* 233 (1999) 21.
- [2] N. Balaban, A. Rasooly, *Int. J. Food Microbiol.* 61 (2000) 1.
- [3] L.R. Boots, S. Potter, D. Potter, R. Azziz, *Fertil. Steril.* 69 (1998) 286.
- [4] R.A. Dudley, P. Edwards, R.P. Ekins, D.J. Finney, I.G. McKenzie, G.M. Raab, D. Rodbard, R.P. Rodgers, *Clin. Chem.* 31 (1985) 1264.
- [5] R.L. Fitzgerald, D.A. Herold, *Clin. Chem.* 42 (1996) 749.
- [6] H. Fukazawa, M. Watanabe, F. Shiraishi, H. Shiraishi, T. Shiozawa, H. Matsushita, Y. Terao, *J. Health Sci.* 48 (2002) 242.
- [7] W. Horwitz, L.R. Kamps, K.W. Boyer, *J. Assoc. Off. Anat. Chem.* 63 (1980) 1344.
- [8] J. Inczedy, T. Lengyel, A.M. Ure, *Compendium of Analytical Nomenclature—The Orange Book*, third ed., Blackwell Science, 1998, ISBN 0-632-05127-2.
- [9] M. Islinger, D. Willmski, A. Volkl, T. Braunbeck, *Aquat. Toxicol.* 62 (2003) 85.
- [10] R.J. Kavlock, G.P. Daston, C. DeRosa, P. Fenner-Crisp, L.E. Gray, S. Kaattari, G. Lucier, M. Luster, M.J. Mac, C. Maczka, R. Miller, J. Moore, R. Rolland, G. Scott, D.M. Sheehan, T. Sinks, H.A. Tilson, *Environ. Health Perspect.* 104 (1996) 715.
- [11] D.G.J. Larsson, M. Adolfsson-Erici, J. Parkkonen, M. Pettersson, A.H. Berg, P.-E. Olsson, L. Forlin, *Aquat. Toxicol.* 45 (1999) 91.
- [12] V.R. Meyer, *Schweizerische Lab. Zeitschrift.* 60 (2003) 63.
- [13] R.M. Nakamura, F.Z. Stanczyk, in: R.A. Lobo, D.R. Mishell Jr., R.J. Paulson, D. Shoupe (Eds.), *Mishell's Textbook of Infertility, Contraception and Reproductive Endocrinology*, fourth ed., Blackwell Science, Malden, MA, 1997, pp. 76–88.
- [14] G.H. Panter, R.S. Thompson, J.P. Sumpter, *Aquat. Toxicol.* 42 (1998) 243.
- [15] G.A. Parker, *J. Assoc. Off. Anat. Chem.* 74 (1991) 868.
- [16] M. Petrovic, E. Eljarrat, M.J. Lopez de Alda, D. Barcelo, *J. Chromatogr. A* 974 (2002) 23.
- [17] J. Piehler, A. Brecht, T. Giersch, B. Hock, G. Gauglitz, *J. Immunol. Methods* 201 (1997) 189.
- [18] A. Promberger, E.R. Schmid, *Ernährung/Nutrition* 25 (2001) 396.
- [19] C.E. Purdom, P.A. Hardiman, V.J. Bye, N.C. Eno, C.R. Tyler, J.P. Sumpter, *Chem. Ecol.* 8 (1994) 275.
- [20] J. Rose, H. Holbech, C. Lindholm, U. Norum, A. Povlsen, B. Korsgaard, P. Bjerregaard, *Comp. Biochem. Phys. C* 131 (2002) 531.
- [21] E.J. Routledge, D. Sheahan, C. Desbrow, G.C. Brighty, M. Waldock, J.P. Sumpter, *Environ. Sci. Technol.* 32 (1998) 1559.
- [22] H.-M. Schmitt, A. Brecht, J. Piehler, G. Gauglitz, *Biosens. Bioelectron.* 12 (1997) 809.
- [23] L.S. Shore, M. Gurevitz, M. Shemesh, *Estrogen Bull. Environ. Contam. Toxicol.* 51 (1993) 361.
- [24] M.J. Sweeney, S. White, A.D.W. Dobson, *Irish J. Agric. Food Res.* 39 (2000) 235.
- [25] J. Taieb, B. Mathian, F. Millot, M.-C. Patricot, E. Mathieu, N. Queyrel, I. Lacroix, C. Somma-Delpero, P. Boudou, *Clin. Chem.* 49 (2003) 1381.
- [26] K.L. Thorpe, T.H. Hutchinson, M.J. Hetheridge, M. Scholze, J.P. Sumpter, C.R. Tyler, *Environ. Sci. Technol.* 35 (2001) 2476.
- [27] J. Tschmelak, G. Proll, G. Gauglitz, *Talanta* 65 (2005) 313.
- [28] M.A. O'Connell, B.A. Belanger, P.D. Haaland, *Chemometr. Intell. Lab. Syst.* 20 (1993) 97.
- [29] K. Van den Belt, R. Verheyen, H. Witters, *Arch. Environ. Conf. Toxicol.* 41 (2001) 458.
- [30] K. Van den Belt, P.W. Wester, L.T.M. van der Ven, R. Verheyen, H. Witters, *Environ. Toxicol. Chem.* 21 (2002) 767.
- [31] M.J. Wheeler, A. D'Souza, J. Matadeen, P. Croos, *Clin. Chem.* 42 (1996) 1445.
- [32] R.J. Whitley, A.W. Meikle, N.B. Watts, in: C.A. Burtis, E. Ashwood (Eds.), *Tietz Textbook of Clinical Chemistry*, WB Saunders Company, Philadelphia, 1994, pp. 1843–1886.
- [33] F.H. Wians Jr., J. Stuart, *Clin. Chem.* 43 (1997) 1466.
- [34] W.F. Young, P. Whitehouse, I. Johnson, N. Sorokin, R&D Technical Report P2-T04/1, Environment Agency, Bristol, England, 2002.